Nuclear Localization of α-Synuclein and Its Interaction with Histones†

John Goers,‡,§ Amy B. Manning-Bog,⊥ Alison L. McCormack,⊥ Ian S. Millett,# Sebastian Doniach,# Donato A. Di Monte,⊥ Vladimir N. Uversky,*,‡ and Anthony L. Fink*,‡

Department of Chemistry and Biochemistry, University of California, Santa Cruz, California 95064, Department of Chemistry and Biochemistry, California Polytechnic State University, San Luis Obispo, The Parkinson's Institute, Sunnyvale, California 94089, and Departments of Chemistry and Physics, Stanford University, Stanford, California 94305

Received January 21, 2003; Revised Manuscript Received April 24, 2003

ABSTRACT: The aggregation of α-synuclein is believed to play an important role in the pathogenesis of Parkinson's disease as well as other neurodegenerative disorders ("synucleinopathies"). However, the function of α-synuclein under physiologic and pathological conditions is unknown, and the mechanism of α-synuclein aggregation is not well understood. Here we show that α-synuclein forms a tight 2:1 complex with histones and that the fibrillation rate of α-synuclein is dramatically accelerated in the presence of histones in vitro. We also describe the presence of α-synuclein and its co-localization with histones in the nuclei of nigral neurons from mice exposed to a toxic insult (i.e., injections of the herbicide paraquat). These observations indicate that translocation into the nucleus and binding with histones represent potential mechanisms underlying α-synuclein pathophysiology.

Parkinson's disease (PD)[1] is the second most common neurodegenerative disorder, after Alzheimer's disease. Clinically, it is a slowly progressive movement disorder whose symptoms are attributed to the progressive loss of dopaminergic neurons from the substantia nigra. Some surviving nigrostriatal dopaminergic neurons contain cytosolic filamentous inclusions known as Lewy bodies and Lewy neurites, of which the protein α-synuclein is a major component (*1*, *2*).

The cause of Parkinson's disease is unknown, but considerable evidence suggests a multifactorial etiology involving genetic susceptibility and environmental factors (*3*). Recent work has shown that, except in extremely rare cases, there appears to be no direct genetic basis for sporadic Parkinson's disease (*4*). However, several epidemiological studies have implicated environmental factors, especially pesticides and metals. Both metals (*3*, *5*) and pesticides (*3*, *6*, *7*) can accelerate the formation of α-synuclein fibrils in vitro and in an in vivo mouse model. Oxidative stress has been proposed as another factor in PD pathogenesis (*8*, *9*). In addition, malfunctioning of a system preventing precipitation, e.g., chaperones (*10*), and abnormalities of the ubiquitin−proteosome pathway (*11*) are also suspected in promoting α-synuclein aggregation and possible neurodegeneration.

α-Synuclein is a small (14 kDa), highly conserved presynaptic protein with unknown function that is abundant in various regions of the brain (*12*−*15*). This protein has been estimated to account for as much as 1% of the total protein in soluble cytosolic brain fractions (*14*). Initially, α-synuclein was described as a neuron-specific protein localized to the nucleus and presynaptic nerve terminals (*12*). However, most subsequent studies have shown α-synuclein localized only within nerve terminals in the central nervous system (*16*−*18*). Structurally, both α-synuclein and the histones belong to the rapidly growing family of intrinsically disordered or natively unfolded proteins, which have little or no ordered structure under physiological conditions (*19*, *20*), due to a unique combination of low overall hydrophobicity and large net charge (*21*).

In this work, we show that histones form specific complexes with α-synuclein, and that the rate of α-synuclein fibrillation in vitro is dramatically accelerated in the presence of histones. Further, the α-synuclein concentration in the neuronal nucleus is shown to increase significantly soon after toxic insult with the pesticide paraquat. These observations indicate that nuclear localization of α-synuclein may play an important role in the physiology and pathophysiology of this protein.

MATERIALS AND METHODS

Materials. Expression and purification of human recombinant α-synuclein from *Escherichia coli* were performed as previously described (*22*). Thioflavin T (ThT) and bovine histones, type III-S (histone H1) and type II-S (mixture of core histones H2a, H2B, H3, and H4), were obtained from Sigma, St. Louis, MO. All other chemicals were of analytical grade from Fisher Chemicals.

† This work was supported by grants (NS39985, NS40132, and ES10806) from the National Institutes of Health.

* To whom correspondence should be addressed: Department of Chemistry and Biochemistry, University of California, Santa Cruz, CA 95064. Tel: 831-459-2744. Fax: 831-459-2935. E-mail: enzyme@cats.ucsc.edu.

‡ University of California.

§ California Polytechnic State University.

⊥ The Parkinson's Institute.

Stanford University.

[1] Abbreviations: PD, Parkinson's disease; ThT, thioflavin T; PAGE, polyacrylamide gel electrophoresis; CD, circular dichroism; ANS, 8-anilino-1-naphthalene sulfonate; SAXS, small-angle X-ray scattering; EM, electron microscopy; PBS, phosphate-buffered saline; MOM, mouse on mouse monoclonal; TH, tyrosine hydroxylase.

10.1021/bi0341152 CCC: $25.00
Published on Web 06/24/2003

Native and Denaturing Polyacrylamide Gel Electrophoresis (PAGE). Denaturing sodium dodecyl sulfate PAGE (SDS−PAGE) was performed with PhastSystem 8−25% gradient gels (Amersham Biosciences, Piscataway, NJ). Samples of α-synuclein−histone fibrils were separated from soluble proteins by microcentrifugation at 18000*g* for 25 min, washed once with buffer, and boiled for 10 min in 2% SDS prior to SDS−PAGE. Native electrophoresis was performed in 7.5% homogeneous gels for 30 min at 60 V in 0.088 M L-alanine, 0.025 M Tris-HCl pH 8.8. All gels were stained with Coomassie blue.

Stoichiometry of α-Synuclein−Histone Complexes. Histone H1 (1 μM) was titrated with increasing concentrations of α-synuclein at 23 °C in 100 mM NaCl, 20 mM Tris-HCl pH 7.2. Complex formation was monitored by the increase in ANS (0.5 μM) fluorescence (excitation at 350 nm, emission at 480 nm). α-Synuclein does not bind ANS, whereas histone does. However, the ANS fluorescence increases more than 2-fold upon α-synuclein binding to histone.

Circular Dichroism Measurements. CD spectra were obtained on an AVIV 60DS spectrophotometer (Lakewood, NJ) using an α-synuclein concentration of 70 μM at 23 °C in 100 mM NaCl, 20 mM Tris-HCl pH 7.2. Spectra were recorded in 0.01-cm cells from 250 to 190 nm. An average of five scans was obtained for each protein spectrum, followed by subtracting the buffer spectrum and calculating the ellipticity. The α-synuclein−histone spectrum was corrected to show only α-synuclein ellipticity by subtracting the spectrum of free histone.

Small Angle X-ray Scattering Experiments. Small-angle X-ray scattering (SAXS) measurements were made using beam line 4−2 at Stanford Synchrotron Radiation Laboratory as previously described (*19*). Analysis of the scattering curves using the Debye approximation provides the radius of gyration, R_g. Scattering data in the form of Kratky plots provide information about the globularity (packing density) and conformation of a protein (*23*, *24*). $I(0)$, the forward scattering amplitude, is proportional to $n\rho_c^2V^2$, where n is the number of scatterers (protein molecules) in solution; ρ_c is the electron density difference between the scatterer and the solvent; and V is the volume of the scatterer. Thus, $I(0)$ is proportional to the square of the molecular weight of the molecule. This means that $I(0)$ for a pure N-mer will be N-fold that for the same number of monomers since each N-mer will scatter N^2 times as strongly as the monomer, but in this case the number of scattered particles (N-mers) will be N times less than that in the pure monomer sample.

Fibril Formation. The kinetics of fibril formation of α-synuclein in the presence or absence of histones were monitored using a Fluoroskan Ascent fluorescence plate reader as previously described (*22*). Fibrillation was performed at 37 °C with agitation in 100 mM NaCl, 20 mM Tris-HCl, 20 μM thioflavin T (ThT), pH 7.2, holding α-synuclein constant at 70 μM and increasing the histone concentration. ThT fluorescence intensities were plotted as a function of time and fitted to a sigmoidal curve (*25*).

Electron Microscopy. Transmission electron micrographs were collected using a JEOL JEM-100B microscope and Formvar-coated 300 mesh copper grids (Ted Pella Inc., Redding, CA). Samples of 0.5 mg/mL were applied to the grids for four minutes followed by two washings with water and four washings with 1% uranyl acetate.

Animals and Treatment. Male mice (8-weeks old; Simonsen Laboratories) received intraperitoneal injections of saline or 10 mg/kg paraquat dichloride dissolved in saline once a week for three consecutive weeks and were sacrificed by cervical dislocation one week following the last injection. Experimental protocols were in accordance with the NIH guidelines for use of live animals and were approved by the Animal Care and Use Committee at The Parkinson's Institute.

Histochemistry. Following removal from the skull, the brain was dissected coronally at the level of the median eminence. The caudal block was immersion fixed in 4% paraformaldehyde in 0.1 M phosphate-buffered saline, pH 7.4 (PBS) and then cryoprotected in 10% and 30% sucrose. Coronal sections throughout the entire substantia nigra (40 μm) were cryostat-cut. Tissues for bright-field microscopy were incubated overnight in Mouse on Mouse Monoclonal (MOM) blocking reagent (Vector Laboratories) diluted 1:25 in PBS, pH 7.4, followed by anti-α-synuclein (Syn-1; BD-Transduction Labs) diluted 1:200 in MOM protein concentrate solution for 1 h. Sections were rinsed prior to immersion in biotinylated anti-mouse IgG secondary for 1 h, treated with 0.3% H_2O_2 to quench endogenous peroxidase activity, and incubated in avidin−biotin peroxidase complex for 30 min. Immunoreactivity was visualized using 0.03% 3,3′-diaminobenzidine for 3 min. Sections were mounted on gelatin-coated slides, counterstained in 0.5% Cresyl violet, dehydrated, and coverslipped. For confocal microscopy, midbrain sections were incubated overnight in MOM blocking reagent diluted 1:25 in PBS, pH 7.4, and then in either (i) anti-α-synuclein (Syn-1; BD-Transduction Labs) and anti-tyrosine hydroxylase (anti-TH; Pel Freez), (ii) anti-α-synuclein and anti-NeuN (Neuron Specific Nuclear Protein, Chemicon), or (iii) anti-α-synuclein and anti-acetylated histone H3 (US Biological). Dilutions were 1:200, 1:1,000, 1:200, and 1:250 for syn-1, anti-TH, anti-NeuN, and anti-histone H3, respectively, in MOM protein concentrate solution. Control sections were incubated in mouse and rabbit IgG (DAKO) to ensure specificity and showed lack of immunoreactivity. After rinsing, tissues were immersed in anti-mouse IgG conjugated to fluorescein (1:100; Chemicon) and anti-rabbit IgG conjugated to Cy3 (1:100; Chemicon) diluted in 1% bovine serum albumin/0.1% Triton X-100 in PBS (2 h, room temperature). Sections were rinsed in PBS and mounted in Anti-Fade medium (Molecular Probes). Immunoreactivity was observed with a light microscope (Nikon) equipped for epi-fluorescence and by confocal microscopy using the Zeiss-LSM5 Pascal system (Carl Zeiss Microimaging Inc.).

RESULTS

In Vitro Effect of Histones on Oligomerization and Fibrillation of α-Synuclein. The ability of human α-synuclein to form soluble complexes with bovine histones was evaluated by native polyacrylamide gel electrophoresis. Figure 1 shows that increasing histone H1 concentrations result in a progressive accumulation of α-synuclein−histone complexes having mobility intermediate between the two proteins and

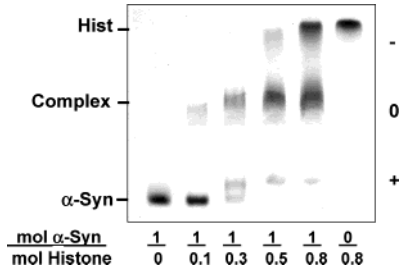

FIGURE 1: Effect of histone H1 on oligomerization and fibrillation of α-synuclein in vitro. Native PAGE of human recombinant α-synuclein (70 μM) in the presence of increasing concentrations of bovine histone H1. The molar ratio of α-synuclein to histone is shown beneath each lane, and the point of sample application is shown as a zero. The sample was applied at the middle of the gel (0) and since α-synuclein and histone are oppositely charged they migrate in opposite directions in the electric field (+, −). The complex has little net charge.

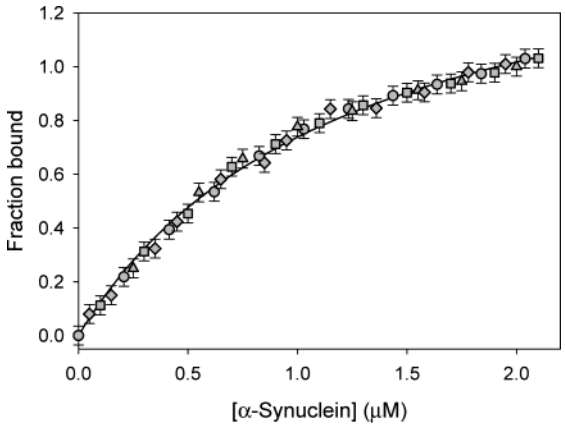

FIGURE 2: The titration of histone H1 (1 μM) with α-synuclein at 23 °C in 100 mM NaCl, 20 mM Tris-HCl, pH 7.2. Complex formation was monitored by the increase in ANS fluorescence (see text). The ANS fluorescence increases more than 2-fold upon α-synuclein binding to histone. ANS concentration was 0.5 μM. The results of four independent experiments are depicted, with the results of different experiments being marked by different symbols. Analysis of the binding data revealed that the stoichiometry of α-synuclein binding to histone H1 is 1.73 ± 0.05, and K_a = 1.29 ± 0.08 × 10^6 M.

an apparent dissociation constant of ≤ 1 μM. Complex formation appeared complete when sufficient histone was added to provide approximately two α-synuclein molecules for every one histone molecule. Similar affinities and stoichiometries were obtained with bovine core histones (data not shown). α-Synuclein−histone H1 complex formation was further verified by spectrofluorometric titration (Figure 2) and by SAXS analysis (see below).

Confirmation of the stoichiometry and affinity of α-synuclein/histone complex formation was obtained from titration of histone H1 with α-synuclein, monitored by ANS fluorescence, Figure 2. We have established that the ANS fluorescence increases more than 2-fold upon α-synuclein binding to histone H1. This observation has been used to evaluate the binding parameters of α-synuclein to histone H1: from the titration curve in Figure 2, saturation of histone H1 by α-synuclein, occurs at an α-synuclein to histone H1 ratio of ∼2. The experimental data for the changes in fluorescence intensity were fitted with a theoretical curve computed according to the *n* independent sites binding scheme:

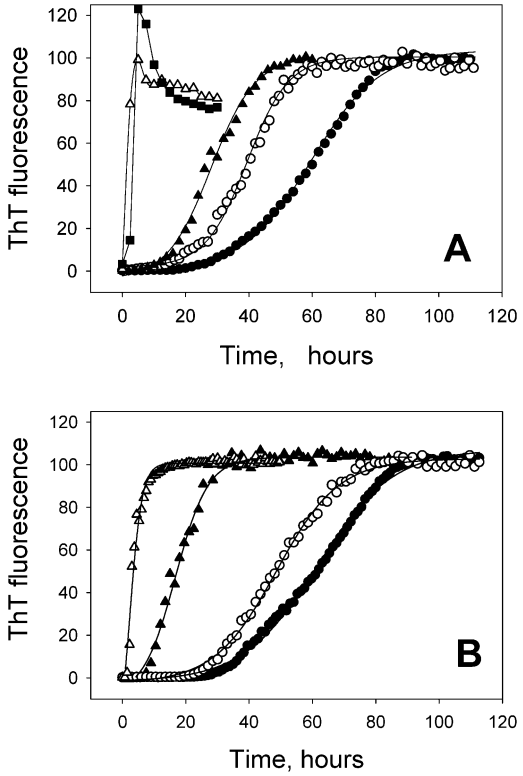

FIGURE 3: Dose-dependent acceleration of α-synuclein (70 μM) fibrillation with increasing concentrations of histone H1 (A) or core histones (B): ● no histone; ○ 0.45 μM; ▲ 4.5 μM; ■ 14 μM; △ 45 μM histone. Fibrillation was monitored by thioflavin T fluorescence.

$$n\ \alpha\text{-synuclein} + \text{histone H1} \leftrightarrows \alpha\text{-synuclein}_n - \text{histone H1}$$

The best fit was achieved with $n = 1.73 \pm 0.05$, and $K_d = 7.7 \pm 0.1 \times 10^{-7}$ M.

The isoelectric points are 4.7 and 11 for α-synuclein and histone, respectively; thus, at neutral pH the two proteins will have opposite net charges. The native gels show that the complex has a net charge of close to zero, suggesting that the interaction between histone and α-synuclein is driven by electrostatic interactions.

To determine whether histones could affect the fibrillation of human α-synuclein, we monitored the rate of fibril formation by the increase in ThT fluorescence in the presence of increasing concentrations of bovine histone H1 (Figure 3A) or bovine core histones (mixture of histones H2a, H2b, H3, and H4, Figure 3B). Solutions of α-synuclein form fibrils over a period of days to weeks, depending on the protein concentration, ionic strength, and the agitation rate of the incubation solution. Under the conditions used in this study (70 μM α-synuclein, 100 mM NaCl), the lag was 30−40 h. Increasing concentrations of histone H1 or core histones significantly accelerated α-synuclein fibrillation in a dose-dependent manner leading to lag times as short as 2 h with 35 μM histone H1, Figure 3A. Core histones showed a similar dose-dependent acceleration of α-synuclein fibril formation (Figure 3B). The underlying basis for the decrease in ThT signal at later times in the two fastest traces in Figure 3A is unclear; however, such phenomena are observed occasionally, even in the absence of histones.

Samples of fibrils formed from α-synuclein−histone mixtures showed incorporation of both proteins into amyloid-

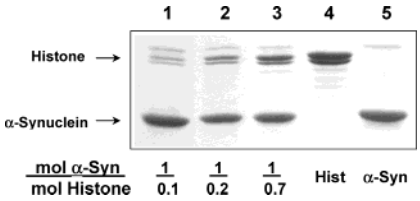

FIGURE 4: SDS−PAGE of α-synuclein fibrils grown in the presence of histone H1. Lanes 1−3: the fraction beneath each lane indicates the molar input ratio of α-synuclein to histone H1 in the initial fibrillation mixture. Lanes 4 and 5 show one molar equivalent of either histone H1 or α-synuclein used in the mixtures.

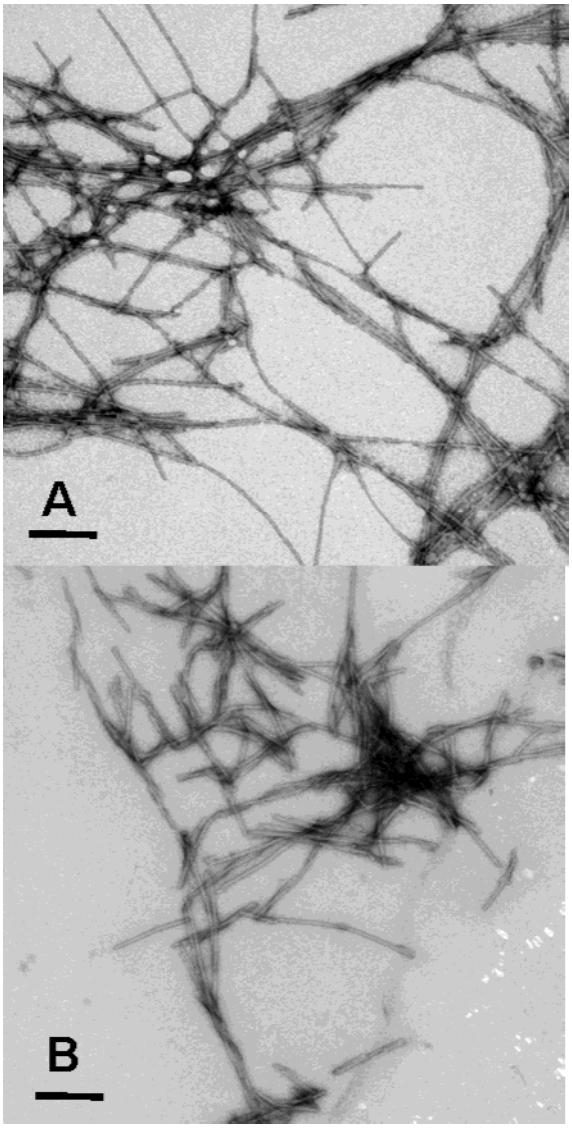

FIGURE 5: Negatively stained transmission electron micrographs of α-synuclein fibrils prepared in the absence (A), or presence of 0.10 molar equivalent of histone H1 (B). The bars indicate 100 nm.

like fibrils. Fibrils were isolated by centrifugation, washed, and analyzed by SDS−PAGE (Figure 4). While 85−95% of the added α-synuclein was incorporated into the fibrils, no more that 50% of the added histone was incorporated, supporting the approximate 2:1 α-synuclein/histone molar ratio seen in the soluble complex of Figure 1.

Interestingly, incorporation of histones into the α-synuclein fibrils was not accompanied by a dramatic change in the

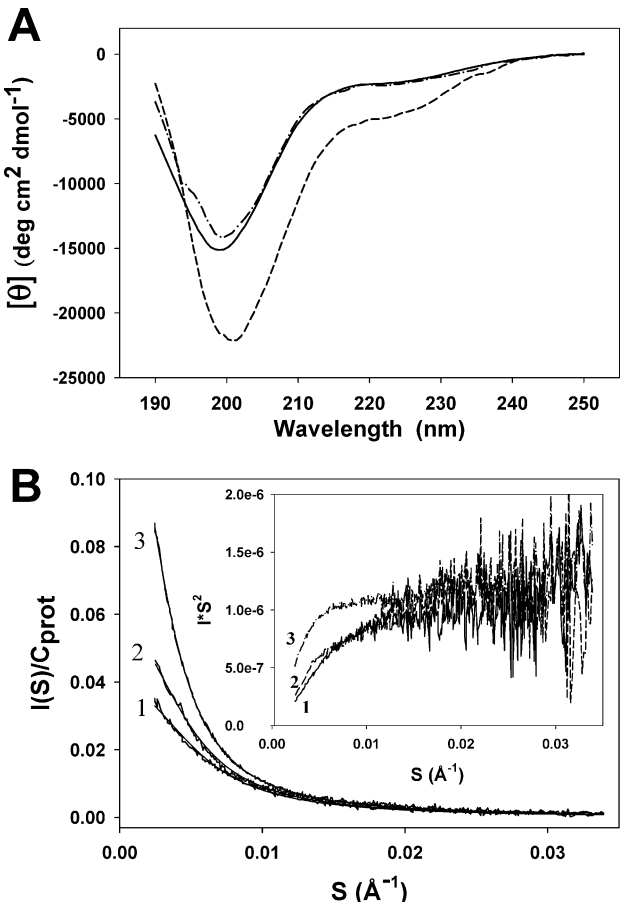

FIGURE 6: Structural characteristics of α-synuclein−histone complex. (A) Far-UV CD spectra of 70 μM α-synuclein measured in the absence (solid line) or presence (dot−dash line) of 35 μM histone (the spectral contribution of the histone was subtracted). Spectrum of histone alone (dash line) is shown for comparison. (B) SAXS spectra (main graph) of α-synuclein (1), histone (2) and α-synuclein-histone complex (3). The dashed lines represent the data fit according to the Debye approximation, but are difficult to see since they are superimposed by the experimental data. The inset shows the Kratky plot analysis of the SAXS results for α-synuclein (1), histone (2), and α-synuclein−histone complex (3).

morphology of fibrils, as seen by electron microscopy (Figure 5). To gain a more complete molecular explanation of this phenomenon, the effect of complex formation on α-synuclein structure was analyzed with two biophysical approaches.

Structural Consequences of α*-Synuclein Binding to Histones.* Circular dichroism spectra provide information about the secondary structure of proteins, while SAXS data provides information on the radius of gyration, packing density, and shape. Figure 6A indicates that both α-synuclein and histone have unfolded structures at neutral pH, as evidenced by CD minima around 200 nm. SAXS data (Figure 6B) indicate that each protein also has a large hydrodynamic radius ($R_g = 46.2 \pm 1.3$ and 53.5 ± 1.6 Å for α-synuclein and histone, respectively), and lacks globular structure (evident from the shape of the Kratky plots, Figure 6B inset). Interestingly, the formation of soluble α-synuclein−histone complexes was not accompanied by significant changes in either secondary or globular structure. For instance, the CD analysis showed minimal change in the α-synuclein−histone spectrum compared to that of α-synuclein alone, after subtraction of the spectrum of histone (Figure 6A). Debye analysis of the SAXS data showed that the α-synuclein−

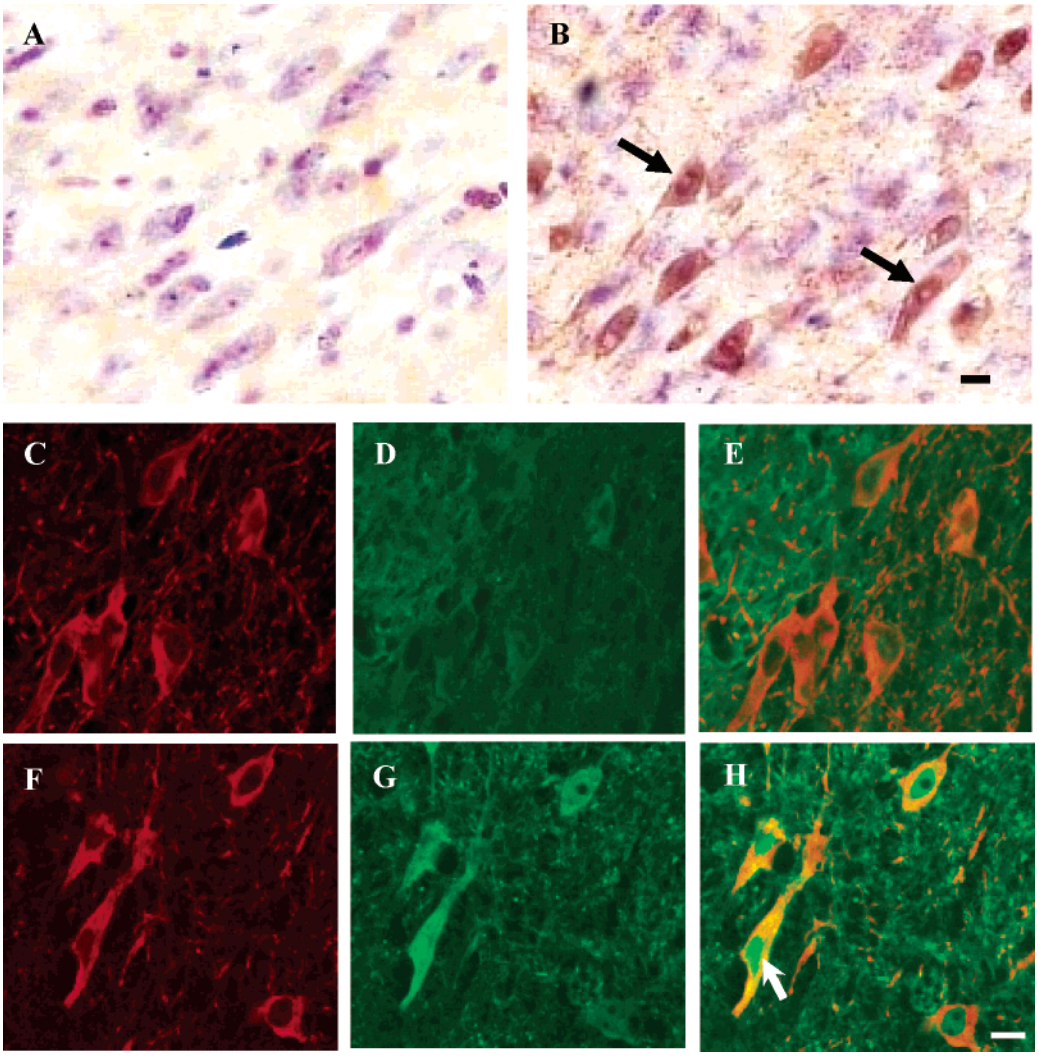

FIGURE 7: Paraquat-induced upregulation of α-synuclein. Midbrain sections from control (A) or paraquat-treated animals (B) were stained for α-synuclein and visualized using bright-field microscopy. Paraquat treatment caused an upregulation of α-synuclein, with intense staining at the levels of both the cytosol and nuclei (arrows in panel B). Midbrain sections from either control (C−E) or paraquat-treated animals (F−H) were double-stained for TH (C,F) and α-synuclein (D,G) immunoreactivities. Comparison of D and G shows increased levels of α-synuclein within nigral cell bodies after paraquat exposure. In tissue from the paraquat-treated mouse, the merged confocal image (H) shows that only α-synuclein immunoreactivity is present at the nuclear level (see arrow), whereas TH and α-synuclein are co-localized in the cytosol. Scale bars = 10 μm.

histone complexes were substantially larger than the monomers (R_g = 76.5 ± 0.8 Å). The apparent molecular masses of α-synuclein, histone, and their complex were calculated from their concentration-normalized $I(0)$ values from SAXS, namely, 0.03872 ± 0.0011, 0.05653 ± 0.0014, and 0.13031 ± 0.0015, respectively. These data indicate that the molecular masses of histone and complex are higher than that of α-synuclein by factors of 1.46 and 3.37, respectively. Thus, the α-synuclein−histone complex has a molecular mass of about 48 700 Da, which corresponds to a stoichiometry of 2:1 (α-synuclein/histone) ($2 \times 14\,460 + 1 \times 21\,000 = 49\,920 \approx 48\,700$) in accordance with estimates from Figures 1 and 2.

Nuclear Localization of α-Synuclein in Vivo. When midbrain sections of control mice were stained with an antibody against α-synuclein, immunoreactivity was diffuse throughout the substantia nigra and stained mostly neuronal fibers (Figure 7A,D). In a recent report, increased levels of α-synuclein were observed within cell bodies of the substantia nigra after exposure of mice to the herbicide paraquat (*6*). We therefore tested the hypothesis that, as a consequence of toxicant-induced upregulation, α-synuclein may be present within nuclei. In paraquat-treated mice, bright field microscopy showed a dramatic increase in α-synuclein immunoreactivity that stained both the cytosol and nuclei of nigral cells (Figure 7B). Sections were also double-stained with antibodies against α-synuclein and TH, a cytosolic marker of dopaminergic neurons. Confocal imaging revealed that, in sections from mice exposed to paraquat, TH, and α-synuclein were co-localized within the cytosol (Figure 7F−H). Merged images also showed, however, that only α-synuclein immunoreactivity was present at the nuclear level (Figure 7H). Nuclear localization of α-synuclein was further demonstrated by co-staining midbrain sections with either (i) anti-α-synuclein and anti-NeuN, a specific marker of neuronal nuclei (Figure 8A−C), or (ii) anti-α-synuclein and anti-acetylated histone 3, a posttranslationally modified histone that is only present within the nucleus (Figure 8D−F). Merged confocal images showed a clear overlap of α-synuclein immunoreactivity with NeuN staining as well as acetylated histone 3 labeling in a sub-population of nigral cells (Figure 8C,F).

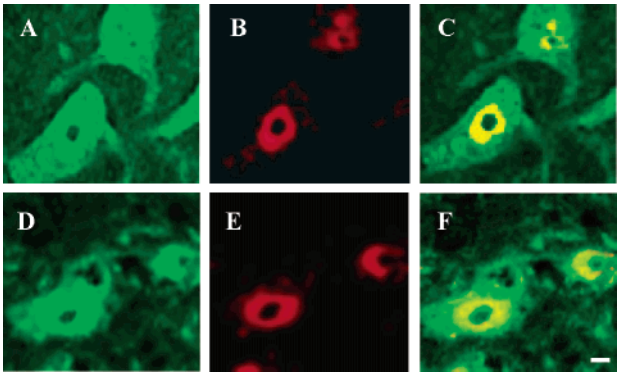

FIGURE 8: Nuclear localization of α-synuclein following paraquat exposure. Midbrain sections from a mouse injected with paraquat were double stained for either NeuN and α-synuclein (A−C), or acetylated histone H3 and α-synuclein (D−F) immunoreactivities. The merged confocal images (C,F) demonstrate co-localization of α-synuclein with the two specific nuclear markers. Scale bar = 10 μm.

DISCUSSION

The pathological hallmark of Parkinson's disease is nigrostriatal degeneration. An additional pathological feature is the presence of intracellular inclusions, Lewy bodies and Lewy neurites, in the dopaminergic neurons of the substantia nigra, as well as neurons in other brain regions. Filamentous α-synuclein has been shown to be the major component of these deposits (*26*−*28*). This observation, in conjunction with the correlation between mutations in α-synuclein and early-onset familial Parkinson's disease (*29*, *30*), strongly suggests that the aggregation of α-synuclein plays a critical role in Parkinson's disease and related neurodegenerative disorders. Although the etiology of Parkinson's disease is unknown, it is most likely to be multifactorial (*3*). Thus, aggregation of α-synuclein triggered by environmental and endogenous factors may be one possible common feature of different mechanisms leading to Parkinson's disease. Our results suggest that one of the endogenous factors promoting α-synuclein aggregation could be the abundant nuclear proteins, histones.

In this study, incubation of α-synuclein with histones in vitro resulted in the formation of stable complexes, characterized by a dissociation constant of about 1 μM and a stoichiometry of 2:1 α-synuclein to histone. While α-synuclein−histone complex formation was not accompanied by significant structural perturbations in these natively unfolded proteins, fibrillation of α-synuclein was dramatically accelerated in the presence of histones, and the latter were incorporated into the fibrils. This acceleration probably reflects histones (containing many positively Arg and Lys residues) acting as scaffolds to bring together molecules of α-synuclein (containing a C-terminal domain enriched in acidic residues) by simple electrostatic interaction. This may then lead to an increase in the effective α-synuclein concentration, known to accelerate fibrillation of this protein (*6*).

The pathophysiologic implications of histone-induced α-synuclein aggregation are not clear at the present time. Lewy bodies in Parkinson's disease are found in the cytosol and not in the nucleus, suggesting that histone−α-synuclein interactions may not underlie the development of these typical inclusions. On the other hand, α-synuclein-containing aggregates have been observed in the nuclei of transgenic mice that overexpress α-synuclein (*31*), indicating that the ability of histones to promote aggregation in vitro may contribute to pathological changes in mice in vivo. That histone−α-synuclein interactions are likely to play an important role in both physiologic and pathologic conditions is also suggested by our present findings in mice treated with the herbicide paraquat. Paraquat administration triggers an upregulation of α-synuclein in the mouse brain that has been interpreted as part of the response of neurons to toxic insults (*6*). We now show that paraquat-induced injury is accompanied by immunohistochemical evidence of nuclear localization of α-synuclein. Indeed, while the nuclei of nigral neurons lack α-synuclein immunoreactivity in normal mice (i.e., animals injected with saline), they do stain with an α-synuclein antibody in mice injected with paraquat. Furthermore, co-localization of α-synuclein with NeuN and histone H3, two specific nuclear markers, is consistent with the possibility that, following paraquat-induced neuronal insult, α-synuclein is translocated into the nuclei where it may interact with histones. Nuclear translocation of α-synuclein and formation of histone−α-synuclein complexes could provide a mechanism by which α-synuclein-related neuronal response may be activated or sustained. In particular, α-synuclein−histone complexes could have a regulatory role by decreasing the pool of free histones available for DNA binding. The subsequent destabilization of nucleosome and enhanced manifestation of the DNA matrix activity could lead to increased transcription and ultimately production of proteins in response to a variety of stimuli, including toxic insults. In this regard, it is interesting to note that elevated levels of the synucleins, especially γ-synuclein, have been associated with ovarian and breast cancers (*32*) and that the expression of γ-synuclein in breast tumors is a marker for tumor progression (*33*).

REFERENCES

1. Lewy, F. H. (1912) in *Handbuch der Neurologie* (Lewandowski, M., Ed.) pp 920−933, Springer, Berlin.
2. Forno, L. S. (1996) *J. Neuropathol. Exp. Neurol. 55*, 259−272.
3. Uversky, V. N., Li, J., Bower, K., and Fink, A. L. (2002) *Neurotoxicology 23*, 527−536.
4. Tanner, C. M., Ottman, R., Goldman, S. M., Ellenberg, J., Chan, P., Mayeux, R., and Langston, J. W. (1999) *JAMA 281*, 341−341.
5. Uversky, V. N., Li, J., and Fink, A. L. (2001) *J. Biol. Chem. 276*, 44284−44296.
6. Manning-Bog, A. B., McCormack, A. L., Li, J., Uversky, V. N., Fink, A. L., and Di Monte, D. A. (2002) *J. Biol. Chem. 277*, 1641−1644.
7. Uversky, V. N., Li, J., and Fink, A. L. (2001) *FEBS Lett. 500*, 105−108.
8. Jenner, P., and Olanow, C. W. (1998) *Ann. Neurol. 44*, 72−84.
9. Yoritaka, A., Hattori, N, Uchida, K., Tanaka, M., Stadtman, E. R., and Mizuno, Y. (1996) *Proc. Natl. Acad. Sci. U.S.A. 93*, 2696−2701.
10. Auluck, P. K., Chan, H. Y., Trojanowski, J. Q., Lee, V. M., and Bonini, N. M. (2002) *Science 295*, 865−868.
11. Johnson, W. G. (2000) *J. Anat. 196 (Pt 4)*, 609−616.
12. Maroteaux, L., Campanelli, J. T., and Scheller, R. H. (1988) *J. Neurosci. 8*, 2804−2815.
13. Jakes, R., Spillantini, M. G., and Goedert, M. (1994) *FEBS Lett. 345*, 27−32.
14. Iwai, A., Masliah, E., Yoshimoto, M., Ge, N., Flanagan, L., de Silva, H. A., Kittel, A., and Saitoh, T. (1995) *Neuron 14*, 467−475.
15. George, J. M., Jin, H., Woods, W. S., and Clayton, D. F. (1995) *Neuron 15*, 361−372.

16. Clayton, D. F., and George, J. M. (1998) *Trends Neurosci. 21*, 249−254.
17. Lavedan, C. (1998) *Genome Res. 8*, 871−880.
18. Clayton, D. F., and George, J. M. (1999) *J. Neurosci. Res. 58*, 120−129.
19. Uversky, V. N., Li, J., and Fink, A. L. (2001) *J. Biol. Chem. 276*, 10737−10744.
20. Weinreb, P. H., Zhen, W., Poon, A. W., Conway, K. A., and Lansbury, P. T., Jr. (1996) *Biochemistry 35*, 13709−13715.
21. Uversky, V. N., Gillespie, J. R., and Fink, A. L. (2000) *Proteins 41*, 415−427.
22. Uversky, V. N., Yamin, G., Souillac, P. O., Goers, J., Glaser, C. B., and Fink, A. L. (2002) *FEBS Lett. 517*, 239−244.
23. Glatter, O., and Kratky, O. (1982) in *Small-Angle X-ray Scattering*, p 515, Academic Press, London, New York.
24. Doniach, S. (2001) *Chem. Rev. 101*, 1763−1778.
25. Nielsen, L., Khurana, R., Coats, A., Frokjaer, S., Brange, J., Vyas, S., Uversky, V. N., and Fink, A. L. (2001) *Biochemistry 40*, 6036−6046.
26. Spillantini, M. G., Crowther, R. A., Jakes, R., Hasegawa, M., and Goedert, M. (1998) *Proc. Natl. Acad. Sci. U.S.A. 95*, 6469−6473.
27. Goedert, M. (2001) *Nat. Rev. Neurosci. 2*, 492−501.
28. Iwatsubo, T., Yamaguchi, H., Fujimuro, M., Yokosawa, H., Ihara, Y., Trojanowski, J. Q., and Lee, V. M. Y. (1996) *Am. J. Pathol. 148*, 1517−1529.
29. Polymeropoulos, M. H., Lavedan, C., Leroy, E., Ide, S. E., Dehejia, A., Dutra, A., Pike, B., Root, H., Rubenstein, J., Boyer, R., Stenroos, E. S., Chandrasekharappa, S., Athanassiadou, A., Papapetropoulos, T., Johnson, W. G., Lazzarini, A. M., Duvoisin, R. C., Di Iorio, G., Golbe, L. I., and Nussbaum, R. L. (1997) *Science 276*, 2045−2047.
30. Kruger, R., Kuhn, W., Muller, T., Woitalla, D., Graeber, M., Kosel, S., Przuntek, H., Epplen, J. T., Schols, L., and Riess, O. (1998) *Nat. Genet. 18*, 106−108.
31. Masliah, E., Rockenstein, E., Veinbergs, I., Mallory, M., Hashimoto, M., Takeda, A., Sagara, Y., Sisk, A., and Mucke, L. (2000) *Science 287*, 1265−1269.
32. Bruening, W., Giasson, B. I., Klein-Szanto, A. J., Lee, V. M., Trojanowski, J. Q., and Godwin, A. K. (2000) *Cancer 88*, 2154−2163.
33. George, J. M. (2002) *Genome Biol. 3*, reviews 3002.1−3002.6.

BI0341152